JOURNAL OF MATERIALS SCIENCE 33 (1998) 4029–4033

Radiographic inspection of reaction-sintered discontinuously reinforced Al–Si alloy composites

J. U. EJIOFOR, R. G. REDDY
Dept. of Metallurgical and Materials Engineering, The University of Alabama, P.O. Box 870202, Tuscaloosa, AL 35487, USA

G. F. FERNANDO
Dept. of Materials Technology, Brunel, The University of West-London, Uxbridge, Middlesex, UB8 3PH, UK
E-mail: rreddy@coe.eng.ua.edu

Detection and identification of defects and reinforcement phases in reaction-sintered hypereutectic Al-13.5Si-2.5 Mg alloy composites was studied using X-ray radiation. Both the coconut shell char-reinforced and zircon sand-reinforced alloy composites revealed cavities due to thermal defects, gas pores, and voids. The low-density char particles were not detected, but the high-density zircon particulates appeared as dark inclusions on the exographs and this offers a good visual measure of particle dispersion in the liquid-phase sintered parts. At the same conditions of irradiation, the low-density Al-Si alloy composites containing high-density zircon particles did not reveal any clear images. Clusters of alumina-silica short fibres as well as line defects appeared bright but their nature was not discernible, making it difficult to identify the defects in the radiographs.

1. Introduction

The commercialization of aluminium metal matrix composites (AMC) is fast increasing as investors seek to reduce materials and production costs while developing high performance, lower weight, structural materials [1]. However, while the non-destructive evaluation (NDE) of monolithic metallic materials has continued to attract the interest of investigators [2, 3], parallel efforts have not been undertaken in NDE of the emerging discontinuously reinforced-composite materials for detection and identification of flaws. Most of the available studies [4–6] have been focused on polymer-based composites. Composites have various kinds of flaws built into them during the manufacturing process, and similar looking ones (on surface visual appearance) may have quite different properties depending upon their internal features.

Most of the discontinuously reinforced AMC contain low cost, poor thermal conductivity, and low coefficient of expansion ceramic particles or short fibres such as graphite, alumina, carbon chars, silicon carbide, and zircon. These reinforcements (some of which are denser than many commercial aluminium alloys) confer high anisotropy, high acoustic attenuation as well as high thermal stresses and defects due to thermal mismatch with the aluminium alloy matrices in the composites. Both solidification processing and the powder technique are common fabrication methods for the composites. While both methods are known to produce voids at the interfaces when good wetting between the matrix and the reinforcement is lacking, the reaction-sintered parts, without any post-consolidation processing, are more prone to voids, pores and dimensional changes even after the consolidation stage [17]. Also, the homogeneous distribution of the filler phase in the matrix is critical to a sound composite part, and the currently common means of evaluating the distribution is by optical metallography.

The increased reliance on NDE by a wide range of industries is being fueled by the growing and well documented emphasis on quality assurance, process control, in-service monitoring and life prediction [7]. Among the various methods of NDE, radiography, ultrasonic and magnetic testing are popular in detecting defects within a component or structure. Although X-ray inspection cannot identify discontinuities parallel to the direction the radiation is travelling and the cost of the inspection is relatively high, the inspection of relatively simple small parts can be accomplished using only a fraction of each piece [8]. Martin [9] used low energy X-rays to measure the resin content in carbon/epoxy composites, but concluded on the basis of the results that the use of the X-ray adsorption technique for measuring composite resin content is not feasible. Harris [10] has earlier claimed that radiography of composites can be used to identify voids and that thermal cracks cannot be distinguished. However, Prakash [6] suggested that thermal cracks are readily detected, as are foreign objects and inclusions. While Salkind [11] was unable to find void or crack indications in his tests, Nevadunsky *et al.* [12] were able to

detect large voids, porosity, and cracks in adhesives. Although these studies work in non-metallic systems, the apparent disagreement in results reported deserves investigative attention. In addition, attempts to investigate the detection of reinforcements in metal matrix composites have not been published in the literature.

The present work aims to investigate the detection and identification of processing defects as well as the discontinuous ceramic reinforcements incorporated into a hypereutectic aluminium-silicon alloy. A low-cost fabrication method of reaction sintering was adopted for making the composites. The low density carbon char particles, medium density alumina-silica short fibres (saffil), and the high density zircon sand particles used as filler phases were introduced at various volume fractions.

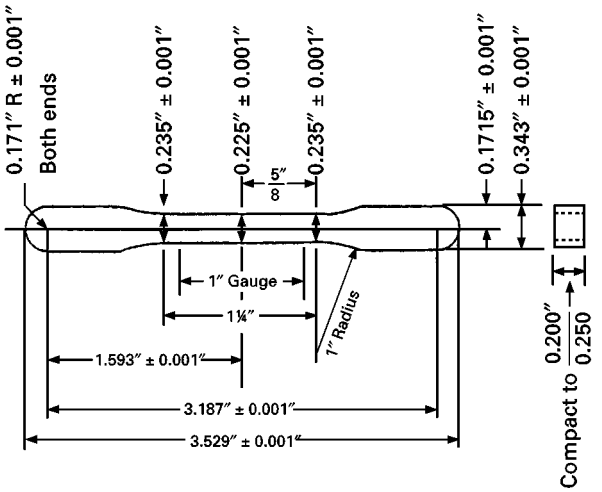

Figure 1 Schematic representation of shape and specifications of the sample parts.

2. Experimental procedure

The unreinforced alloy, Al-13.5Si (composition in wt %), and the composites used in this study were prepared by reaction-sintering of blended elemental powders. The details of the fabrication procedure are given elsewhere [13], and only a brief description is presented here. The matrix is the hypereutectic alloy with small amounts of magnesium as a co-sinter, Al-13.5Si-2.5Mg. The composites, C1 to C3 (C-series), contain various amounts of milled coconut shell char particles (size: $<140\,\mu m$) ranging from 4, 8 to 12 vol %, respectively. Compositional analysis of the char using a CEC 240XA elemental analyser yielded the following in weight per cent: 77.15% C, 2.88% H, 0.24% N, 0.018% P, <0.1% S and others, 19.7%. The Z1 to Z3 (Z-series) composites contain ground zircon particles (size: $<200\,\mu m$) ranging from 9, 12 to 15 vol %, respectively, while F1 to F3 (F-series) are short fibre (Saffil: Al_2O_3/4 wt % SiO_2, density: 3.3 to 3.5 $g\,cm^{-3}$, length: 1.5 mm, nominal diameter: 0.003 mm) reinforced composites with the fibre vol % of 0.3, 0.9 and 1.2, respectively. Although low loadings of reinforcement was used in this case, their clusters were dispersed in order to promote defects in the final parts.

The chemical composition of the zircon sand is (in wt %): 62.12% ZrO_2, 33.13% SiO_2, 2.01% Fe_2O_3, 1.82% HFO_2, 0.58% TiO_2, and others, 0.34%. Stearic acid (size: 500 μm) in the amount of 1 wt % was used to aid compaction. A die-wall lubrication using 0.5 wt % aluminium stearate was also applied to reduce the stripping pressure of the compacts from the hardened steel mould. While the C-series were cold-pressed at 250 MPa, Z-series and F-series were compacted at 350 MPa. Fig. 1 shows the schematic representation of the shape and specifications of the sample parts. The specimens have gauge lengths of uniform thickness, and grip ends of larger thickness. Consolidation of the green parts was carried out in vaccum at temperatures between 580 °C and 620 °C for times that vary from 10 min to 2 h in order to generate shrinkages and other possible defects in the sintered parts.

Density measurements of the particles were made by mercury porosimetry. Because magnesium forms an amalgam with mercury, the densities of the sintered parts were measured using light paraffin oil. This colourless liquid has a kinematic viscosity (at 37.8 °C) of not more than 30 centistoke. The method of radiography was used to examine the distribution of the particulate and short fibres as well as the presence of voids and defects in the sample parts. The Macrtank-K X-ray set with a Hewlett Packard Faxitron Contact Radiography camera was used for this testing. A voltage of 80 kV, current of 5 mA and an irradiation time of 5 min were applied because of the non-uniformity of the thickness of the samples. Source to (flexible) film distance of 70 cm was maintained and the slow, high-contrast, very fine-grain Mx Kodak film grade was used. Lead screen placed in direct contact behind the film was utilized as the intensifier to increase the sharpness of the radiographs.

3. Results and discussion

3.1. Contrast and defects

The primary X-ray beam was focused on the gauge lengths (which is the region of interest) and this explains the sharp contrast revealed by the exographs between this section and the thicker ends. The dosage absorbed by the parts because of the voltage and exposure time (5 min) used (80 kV) produced a, a good definition of the images as could be observed. In addition, lower speed, fine-grained films are known to give high contrast, better definition radiographs. However, radiographing a specimen of non-uniform thickness with one exposure on one film reproduces the thick parts as low densities on the film, and (because film gradient varies directly as film density) there will be a loss of flaw sensitivity in those low densities compared with a normal-density radiograph of these sections [16]. At the other end, the thin sections will be reproduced as high film densities which soon reach the stage of being too high to be viewed. Figs 2 to 4 are the exographs of C-series, Z-series and F-series, respectively, with visually observable distortions along their lengths. Large dimensional changes on reaction-sintered products are known to result from both shrinkage and growth

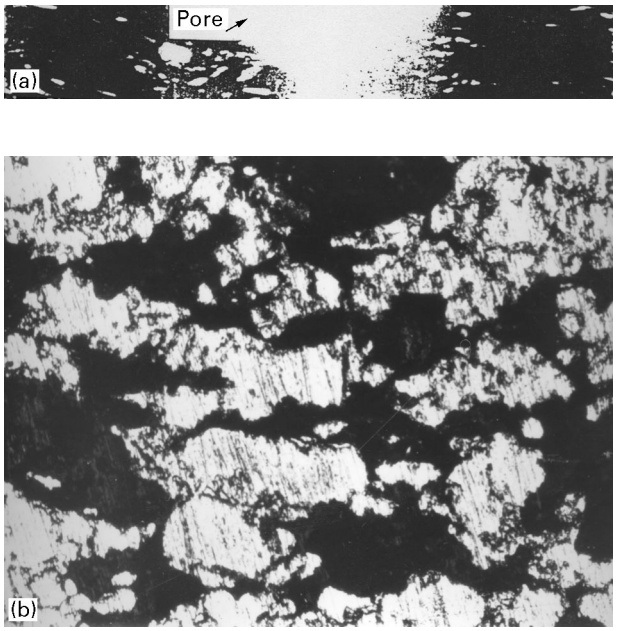

Figure 2 (a) Radiograph of unreinforced Al-13.5Si alloy, and (b) optical micrograph of the alloy revealing porosities (dark); magn: 400 ×.

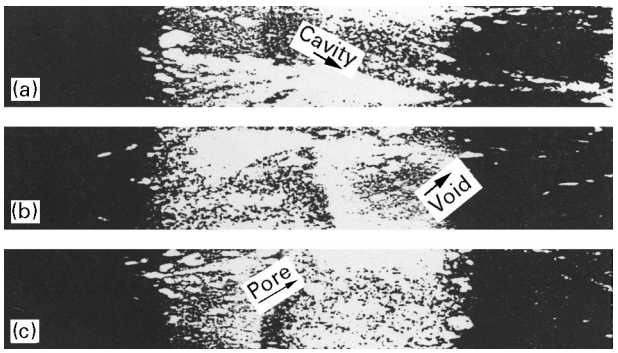

Figure 3 Radiographs of reinforced Al-13.5Si-2.5Mg alloy containing (a) 4 vol % (b) 8 vol % and (c) 12 vol % coconut shell chars. Cavities and elongated porosities (bright) are revealed.

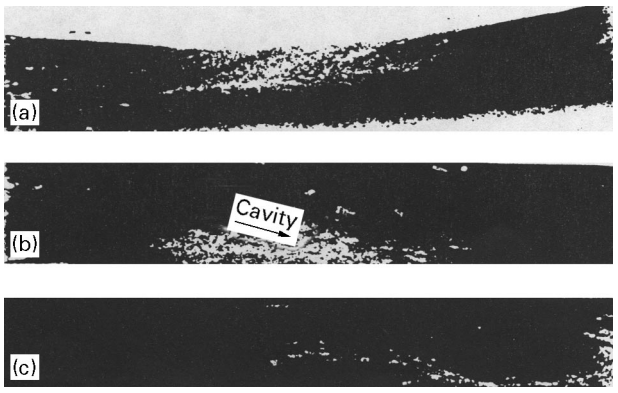

Figure 4 Radiographs of reinforced Al-13.5Si-2.5Mg alloy containing (a) 9 vol % (b) 12 vol % and (c) 15 vol % zircon particles, revealing low amount of defects.

phenomena. While shrinkage is believed to be influenced by surface tensions, chemical reactions, recrystallization processes and increasing attraction and consequent closer contact between the particulate, growth (that is a decrease in apparent density during the sintering process) is controlled by the gas content of the green parts. Kehl *et al.* [14] earlier observed more distortions in internally lubricated sintered parts than in die-wall lubricated and in unlubricated parts. The observed distortions in our discontinuously-reinforced composites therefore may have been due to four factors: lubrication, differing thermal behaviours of the reinforcements and matrix, poor die-filling and poor consolidation conditions. In this consideration, defects such as voids, porosities, thermal cracks and segregation are apparent in our composites.

3.2. Particulate composites and defects

The determined density of the unreinforced alloy is 78% of the theoretical. Shown in Fig. 2a is the radiograph of the alloy. The delubrication and sintering stages have created pores left by the gasified lubricants. These pores (bright in appearance) are revealed in the figure and are aligned in a direction normal to the applied pressure, showing the shape deformation of the lubricants. An optical micrograph of the alloy showing some of the elongated pores is shown in Fig. 2b. It is possible that some matrix particles may have welded together appearing as large bright spots in the exographs, especially when it is noted that aluminium and silicon are of low atomic numbers. All of these can be seen to align transversely to the pressure direction. While C-series and F-series did not consolidate by liquid phase sintering, the zircon-reinforced parts did. The char-reinforced composites shown in Fig. 3a to c reveal both voids and porosities (rounded bright spots). Nevadusky *et al.* [12] have earlier detected large voids, cracks and porosities in adhesives. Discontinuities, in the form of pipes in the composites matrix, due to a swelling effect, could also be observed. On the other hand, the char particles as well as reinforcement segregation are not revealed. Because of the low atomic numbers of carbon and nitrogen, the low density char particles ($0.89\,g\,cm^{-3}$) did not absorb much of the primary radiations and therefore are not reproduced on the film.

Zircon reinforced composites (Fig. 4a to c) of more than 82% density of theoretical were produced. Although blackening of the film occurred due to poor irradiation (and this was due to the difficulty in sharpening the effects due to particulate density and part thickness variations), porosites or voids are not readily revealed in these exographs. In Fig. 5 is shown the optical micrograph of the alloy reinforced with 15 vol % zircon particulate, revealing few porosities only around the coarse-sized zircon particles. This is not only because the population of defects is small but also the high density zircon particulate (theoretical density, about $4.33\,g\,cm^{-3}$) resulted in radiation attenuation. This event reduced any sharp contrast on the film due to any defects. Absence of macroscopic defects, such as porosities, is expected in parts with good sintering aid and consolidated by liquid phase sintering [15]. Under liquid phase sintering, thermal transport of atoms by surface diffusion, bulk diffusion

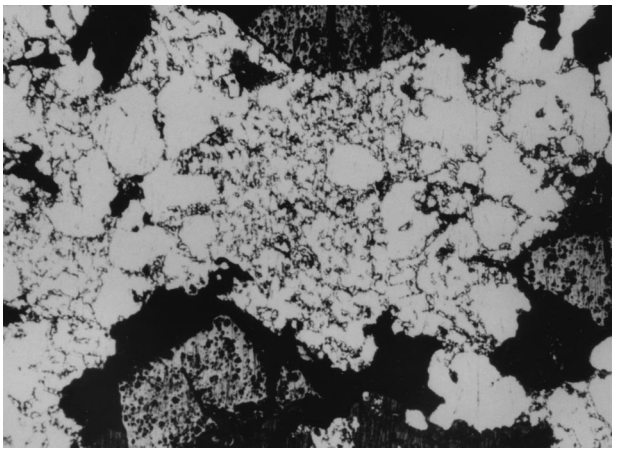

Figure 5 Optical micrograph of Al-13.5Si-2.5Mg alloy containing 15 vol % zircon. Few porosities are present around the coarse-sized particles; magn: 50 ×.

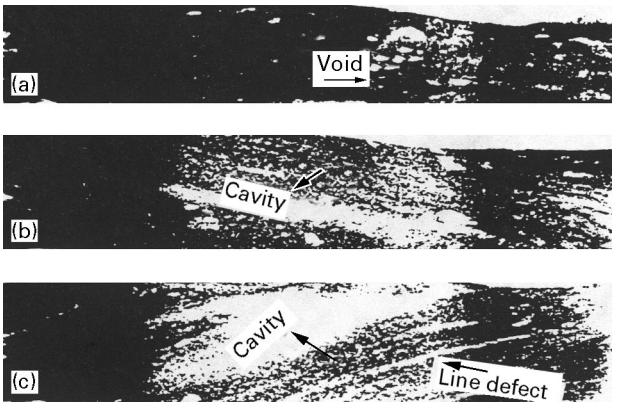

Figure 7 Radiographs of reinforced Al-13.5Si-2.5Mg alloy containing (a) 0.3 vol % (b) 0.9 vol % and (c) 1.2 vol % alumina-silica short fibres. Cavities and line defects can be seen.

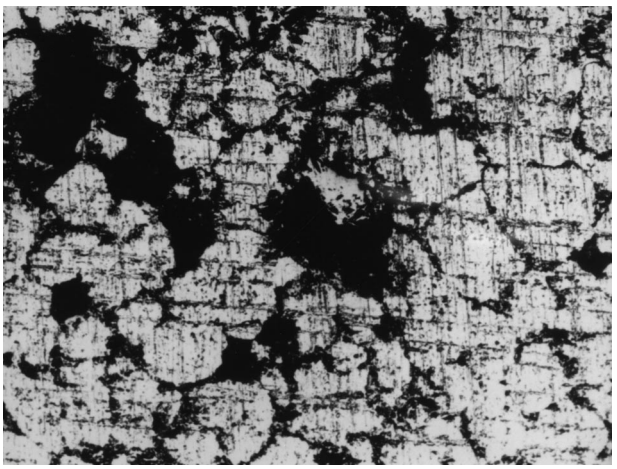

Figure 6 Optical micrograph of Al-13.5Si-2.5Mg alloy containing 12 vol% zircon sectioned at the region with cavity. Porosites (dark) are revealed with no particle; magn: 400 ×.

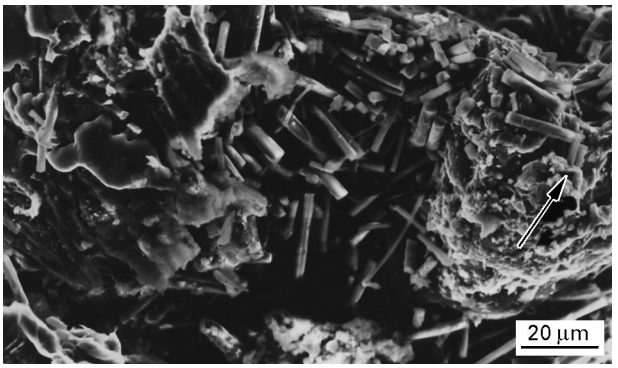

Figure 8 Scanning electron micrograph of swollen section of 1.2 vol % alumina-silica short fibre reinforced Al-13.5Si-2.5Mg alloy. Fibre clusters and open cavities are clearly revealed.

and grain boundary diffusion are promoted, resulting in closing of porosities by the vacancy mechanism [15]. Here, particles of zircon appear very dark and could be seen to be uniformly distributed in the test specimen.

These observations, which revealed only zircon sand and no coconut shell char particles, have refined the report by Prakash [6]. Prakash had earlier concluded that foreign objects and inclusions are readily detectable by the X-ray method. Large localized regions of material discontinuities due to the interplay of swelling and shrinkage as well as to non-uniform die-filling also appear bright (Fig. 4b). A section of this portion was prepared metallographically, and the micrograph is shown in Fig. 6. The voids are dark with no particle present in them.

3.3. Discontinuous fibre composites and defects

Bright features appear in the short fibre composites (Fig. 7a to c). The individual strands of the alumina-silica short fibres (density: 3.3–3.5 g cm^{-3}) are not revealed in the low fibre volume fraction (0.003) composites. Fibre strands aligned parallel to the beam direction appear dark in films due to reduced attenuation [18]. Crane *et al.* [4] were able to radiographically identify boron fibres in polymer-based composites only when the fibres were dusted with a flourescent dye-powder. Thermal cracks, observed on visual inspection, lying across the X-ray beam and nearly traversing the specimen thickness could also be observed (Fig. 7c). This observation, while agreeing with the report by Prakash [6] on metal composites, contradicts earlier findings by Harris [10] on resin-bonded composites. While Prakash observed that specially-oriented thermal cracks are readily detected, Harris had earlier reported that radiography can be used to identify voids, but fibre resin debonding or cracks resulting from thermal contraction cannot be identified. Clusters of the short fibres in the 0.009 and 0.012 V_f composites are not clearly revealed, but appear like cavities in the exographs (Fig. 7b and c). This was discovered when the swollen region in the part shown in Fig. 7c was sectioned, polished and examined under the scanning electron microscope. The micrograph is shown in Fig. 8. It was also observed that the matrix-fibre bonding which occurred along the periphery of the clusters with the matrix was not

extended to the cluster centre due, probably, to restricted powder flow. This resulted in a large shrinkage cavity (dark, in the secondary electron image) in the portion.

The above observations seem to suggest a contrasting behaviour of thermally-synthesized polymer and metal composites to X-rays.

4. Conclusions

The use of "slightly hard" X-rays of 80 kV detected high density particulates, discontinuities due to thermal effects, voids and gas pores in the reaction-sintered discontinuously-reinforced Al-13.5Si-2.5Mg alloy composites. In the coconut shell char reinforced composites, the low-density char particles were not detected in the low-density (2.64 g cm $^{-3}$), hypereutectic Al–Si alloy. The liquid-phase sintered zircon-reinforced particulate composites revealed both porosities as well as the zircon particles (which appear dark in the exographs), and this could offer a good measure of particle dispersion in the sintered part. Localized cavities – suspected to arise from the thermal mismatch between the matrix alloy and zircon – were also revealed in this inspection. It is further concluded that the density of the radiographic film used appears reduced when high-density particulates (such as zircon sand) are used as reinforcements in a low-density alloy matrix, than when low-density particles (such as carbon chars) are used. This suggests the use of different irradiation conditions in radiography of composite parts filled with reinforcement phases of differing densities. Both the strands and clusters of fibres used as discontinuous reinforcements is sintered Al-13.5Si-2.5Mg alloy composites were also not detected by this technique. However, the positions of these clusters appeared as bright regions of cavities in the radiographs.

Acknowledgements

The authors are pleased to acknowledge the financial support of this research by National Science Foundation, grant No. DMR-9314016. We would like to thank Professor B. Ralph and Dr M. Edirisinghe, Dept. of Materials Technology, Brunel University, Uxbridge, West-London, for technical contributions in the course of this work.

References

1. J. U. EJIOFOR and R. G. REDDY, *JOM. Min. Met. Mater. Soc.* November (1997) 31.
2. L. GOLDBERG, in paper presented on "Reliability of Magnetic Particle Inspection Performed Through Coatings", *EPRI NP*-5951 (*Electric Power Research Institute*, 1988).
3. K. J. LANGENBERG, P. FELLINGER and R. MARKLEIN, *Res. Nondestruct. Eval.* **2** (1990) 59.
4. R. L. CRANE, F. CHANG and S. ALLINIKOV, *Mater. Eval.* **36** (1978) 69.
5. I. G. SCOTT and C. M. SCALA, *NDT Int.* **15** (1982) 75.
6. R. PRAKASH, *Composites* **11** (1980) 217.
7. R. N. PANGBORN, D. E. BRAY, J. F. COOK, C. D. COWFER and D. M. SCHLADER eds. in Proceedings of the 1991 Pressure and Piping Conference on Applications, Advanced Methods, and Codes and Standards, San Diego, CA, **PVP-Vol. 216, NDE-Vol. 9** (June 1991).
8. G. P. HAYWARD, in "Introduction to Non-Destructive Testing" (NDT Committee of the Inspection Division of the American Society for Quality Control, Milwaukee, WI, 1978) p. 12.
9. B. G. MARTIN, *Mater. Eval.* **35** (1977) 65.
10. B. HARRIS, *Ann. Chim. Sci. Mater.* **5** (1980) 327.
11. M. J. SALKIND, *J. Aircr.* **13** (1976) 764.
12. J. J. NEVADUNSKY, J. J. LUCAS and M. J. SALKIND, *J. Compos. Mater.* **9** (1975) 394.
13. J. U. EJIOFOR, B. A. OKORIE and R. G. REDDY, *J. Mater. Eng. Perform.* **6** (1997) 326.
14. W. KEHL, M. BUGAJSKA and H. F. FISCHMEISTER, *Powder Metall.* **26** (1983) 221.
15. B. F. ALEXANDER and R. W. BALLUFFI, *J. Met.* **2** (1950) 1219.
16. R. HALMSHAW, in "Industrial Radiological Techniques" (Wykeham Publications, London, 1970).
17. J. U. EJIOFOR and R. G. REDDY, *J. Mater. Eng. Perform.* **6** (1997) 785.
18. R. C. O'BRIEN and W. B. JAMES, in "ASM Handbook", Vol. **17** (1990) p. 537.

Received 2 February
and accepted 7 April 1998